

**First-principles study of electronic and structural properties of CuO**

Burak Himmetoglu, Renata M. Wentzcovitch, and Matteo Cococcioni

*Department of Chemical Engineering and Materials Science, University of Minnesota, Minneapolis, Minnesota 55455, USA*

(Received 23 June 2011; published 14 September 2011; publisher error corrected 3 October 2011)

We investigate the electronic and structural properties of CuO, which shows significant deviations from the trends obeyed by other transition-metal monoxides. Using an extended Hubbard-based corrective functional, we uncover an orbitally ordered insulating ground state for the cubic phase of this material, which was expected but, to the best of our knowledge, was not found in the literature. This insulating state results from a fine balance between the tendency of Cu to complete its  $d$ -shell and Hund's rule magnetism. Starting from the ground state for the cubic phase, we also study tetragonal distortions of the unit cell (recently reported in experiments) and identify the equilibrium structure. Our calculations reveal an unexpected richness of possible magnetic and orbital orders, relatively close in energy to the ground state, whose stability depends on the sign and nature of distortion.

DOI: [10.1103/PhysRevB.84.115108](https://doi.org/10.1103/PhysRevB.84.115108)

PACS number(s): 71.15.Mb

**I. INTRODUCTION**

Among the transition-metal oxide (TMO) compounds, CuO shows quite peculiar characteristics. At variance with other TMOs, which crystallize in a cubic rocksalt structure (with possible rhombohedral distortions), it is found to have a lower-symmetry monoclinic cell.<sup>1-3</sup> Similarly to other TMOs, CuO has an antiferromagnetic ground state.<sup>1</sup> However, its Néel temperature ( $T_N \simeq 220$  K) is lower than the (expected) linear trend followed by other TMOs the Néel temperatures of TMOs are observed to increase almost linearly, from MnO ( $T_N \simeq 116$  K) to NiO ( $T_N \simeq 525$  K), with the nuclear charge of the transition metal]. The reduction in  $T_N$  seems to be related to the fact that the monoclinic ground state is stabilized by a Jahn-Teller structural distortion, which yields lower effective exchange interactions compared to the cubic structure.<sup>4</sup>

In spite of the fact that it is not stable, studying the cubic phase of this material is still interesting as a reference point for the characterization of all the electronic mechanisms correlating to structural deformations. In addition, CuO has also been recently considered as a proxy structure for high  $T_c$  superconducting cuprates,<sup>5</sup> to investigate the interplay between “ $d$ ” and “ $p$ ” electrons and for its unconventional, high-temperature multiferroic character.<sup>6</sup> Although cubic CuO, to the best of our knowledge, has not been observed experimentally, a tetragonal phase of CuO (i.e., elongated rocksalt cell along one crystal axis) has recently been deposited on substrates of SrTiO<sub>3</sub> thin films.<sup>7</sup> The tetragonal phase of CuO has become a subject of several theoretical studies based on density functional theory (DFT).<sup>5,8,9</sup> All the DFT studies have predicted, in agreement with the experimental results, a distortion characterized by  $1.1 \lesssim c/a \lesssim 1.3$  (Refs. 5, 8, and 9) (for which the rocksalt cell is elongated along one of the crystal axis). Among possible magnetic configurations, the antiferromagnetic-II configuration (AF-II), characterized by ferromagnetic (111) planes with opposite spins with respect to their neighbors, and the AF-IV configuration, characterized by ferromagnetic (110) planes with opposite spins with respect to their neighbors, compete for minimum energy. A self-interaction corrected density functional (SIC) based study predicts an AF-II ordered ground state with  $c/a \simeq 1.1$ ,<sup>8</sup> while the hybrid density functionals predict an

AF-IV ordered ground state with  $c/a \simeq 1.3$  (Ref. 9) (it is important to remark that the experimental lattice parameter in Ref. 7, for CuO grown on a SrTiO<sub>3</sub> substrate, is lower than the ones used in computational studies obtained with various functionals, therefore a direct comparison of calculated  $c/a$  values needs care). In both studies, a local energy minimum was also identified at  $c/a \simeq 0.9$ . At this local minimum, the magnetic structure was found to be AF-II. DFT +  $U$ , limited only to the AF-II magnetic ordering, yields an equilibrium structure with  $c/a \simeq 1.1$ .<sup>5</sup> In all these studies, the cubic phase (i.e., the limit when  $c/a = 1$ ) is found to be metallic and corresponding to a local peak in the energy. However, as pointed out in other studies,<sup>5</sup> it seems quite unlikely that the insulating structures with  $c/a < 1$  and  $c/a > 1$  are “connected” by a metallic state at  $c/a = 1$ . Instead, an insulating state for the cubic structure seems more reasonable.

In this paper, we revisit the cubic and tetragonal phases of CuO to investigate the underlying mechanism characterizing the electronic, magnetic, and structural properties of this compound using a DFT +  $U$  based corrective functional within the AF-II magnetic order. We find an insulating ground state for the cubic phase of CuO, which was expected but, to the best of our knowledge, not found in the literature. Starting from this insulating ground state for the cubic cell, we also study tetragonal distortions and find an equilibrium structure in agreement with experiments and previous calculations. The properties of this ground state are controlled by an interesting interplay between Hund's rule magnetism and electronic localization. We believe that similar effects could also play an important role in more complex cuprate materials.

The paper is organized as follows: In Sec. II we summarize the DFT +  $U$  method we have used. In Sec. III we discuss the electronic structure of the cubic phase, from DFT and DFT +  $U$  functionals. In Sec. IV, we introduce an extension of the DFT +  $U$  method to include an effective exchange parameter  $J$  (DFT +  $U$  +  $J$ ) and discuss the resulting electronic structure of the cubic phase. In Sec. V we study elongated structures and compare our results with those from the existing literature. Finally, in Sec. VI we summarize our findings and propose some conclusions.

## II. DFT + $U$ METHOD

In this study, we employ the Hubbard-based DFT +  $U$  corrective scheme, originally introduced in Refs. 10–12, that has become one of the most popular choices to study systems characterized by strong electronic correlations. Although not able to capture all the possible correlated ground states, this corrective scheme has proved to be quite versatile in the description of the properties of several transition-metal compounds,<sup>13,14</sup> minerals of the Earth’s interior,<sup>13–18</sup> molecular complexes,<sup>19–22</sup> TMOs,<sup>10,11,23–25</sup> magnetic impurities, and semiconductors.<sup>26</sup> Other corrective schemes have also been successfully used in the literature, including self-interaction corrected density functionals,<sup>27</sup> hybrid density functionals,<sup>28</sup> dynamical mean-field theory,<sup>29</sup> and reduced density matrix functional theory.<sup>30</sup> Among these, DFT +  $U$  has the advantage to present low computational costs<sup>31</sup> and to allow for the efficient calculation of energy derivatives (e.g., forces, stresses, elastic constants, etc.). The scheme is based on the addition of a corrective term, inspired from the Hubbard model, that favors Mott localization of electrons on atomic sites. The total energy functional of DFT +  $U$  can be written as<sup>23</sup>

$$E_{\text{DFT}+U} = E_{\text{DFT}}[n(\mathbf{r})] + E_U[\{n_{mm'}^{I\sigma}\}], \quad (1)$$

where  $E_{\text{DFT}}$  is a standard approximate DFT functional and the Hubbard correction  $E_U$ , according to the simplified functional by Dudarev *et al.*,<sup>32</sup> is given by

$$E_U = \sum_{I,\sigma} \frac{U^I}{2} \text{Tr}[n^{I\sigma}(\mathbf{1} - \mathbf{n}^{I\sigma})]. \quad (2)$$

In the above equation,  $U^I$  is the Coulomb repulsion parameter on atomic site  $I$  (usually applied on the  $d$  states of a transition metal) and the occupation matrices  $\mathbf{n}^I$  are computed as

$$n_{mm'}^{I\sigma} = \sum_{\mathbf{k}\nu} f_{\mathbf{k}\nu}^{\sigma} \langle \psi_{\mathbf{k}\nu}^{\sigma} | \phi_m^I \rangle \langle \phi_{m'}^I | \psi_{\mathbf{k}\nu}^{\sigma} \rangle, \quad (3)$$

where  $\psi_{\mathbf{k}\nu}^{\sigma}$  denote the Kohn-Sham states,  $f_{\mathbf{k}\nu}^{\sigma}$  represent their occupations according to the Fermi-Dirac distribution of their energy, and  $\phi_m^I$  are the atomic orbitals with state index  $m$  and centered on site  $I$  (in this paper we use orthogonalized atomic orbitals, i.e.,  $\langle \phi_m^I | \phi_{m'}^I \rangle = \delta^{IJ}$ ). The representation of occupation matrices in terms of atomic orbitals given in Eq. (3) is not the only possible choice. The same scheme can be used with different sets of wave functions such as Wannier functions<sup>33,34</sup> that may offer a more flexible representation of electronic localization. For the same purpose, a recent work introduced an extension to the functional of Eq. (2) to include intersite terms.<sup>35</sup> While we expect that the inclusion of these terms (especially those between O and Cu) might be important to refine structural properties and to resolve some fine details in the electronic structure, in this paper we neglect them and focus on the atomic (on-site) ones.

In our paper, the on-site Coulomb repulsion parameters  $U^I$ ’s are determined using the linear response approach introduced in Ref. 23. In this paper, we have generalized this approach to include the responses of the  $s$  states of Cu and O treated as a “reservoir” of charge (instead of the neutralizing “background” of Ref. 23). Our results show that inter-site

interactions ( $V$ ) are significantly smaller than on-site ones ( $U$ ) and our approximation is justified.

In many cases, the DFT ground state for TMOs have different properties than the DFT +  $U$  ground state. For instance, DFT +  $U$  could stabilize a magnetic ground state with an insulating gap, while DFT results in a metallic one. Therefore, a more accurate determination of the  $U^I$ ’s should involve a self-consistent procedure, where the linear response computation is repeatedly performed on the DFT +  $U$  ground state, until a convergence in their values is reached.<sup>19,35</sup> This self-consistent procedure proved to be necessary in our study due to the qualitative differences between the DFT and the DFT +  $U$  ground states.

In our calculations, we have used the Perdew-Burke-Ernzherof (PBE)<sup>36</sup> generalized gradient approximation (GGA) functional to model the exchange-correlation energy. The Cu and O atoms are represented by ultrasoft pseudopotentials and the kinetic energy and charge density cutoffs are chosen to be 35 and 280 Ry, respectively. The Brillouin zone integrations are performed using  $8 \times 8 \times 8$  Monkhorst and Pack special point grids<sup>37</sup> and a Methfessel and Paxton smearing of the Fermi-Dirac distribution,<sup>38</sup> with a smearing width of 0.01 Ry. We have also tested other smearing techniques (e.g., Gaussian) and found no quantitative difference between the results obtained. All calculations were performed by using the plane-waves pseudopotential “pwscf” code contained in the QUANTUM ESPRESSO package,<sup>39</sup> where we have implemented the “+ $J$ ” corrections (as discussed in Sec. IV) starting from the existing DFT +  $U$  functional.

## III. DFT AND DFT + $U$ CALCULATIONS IN THE CUBIC PHASE

Previous studies of the cubic phase of CuO, based on GGA functionals, predicted a metallic and a nonmagnetic ground state. While other TMOs are also predicted to be metallic within GGA, they have an antiferromagnetic ground state with ferromagnetic (111) planes of transition-metal ions alternating with opposite magnetization (AF-II). This magnetic order imposes a rhombohedral symmetry to the cell that sometimes produces a distortion. In this paper, CuO is also described with a unit cell of rhombohedral symmetry. The unit cell consists of four atoms, of which the two Cu atoms have opposite spins. We find that the optimized structure has a lattice parameter of 4.256 Å, which we have adopted for the rest of the calculations. The density of states obtained with GGA is shown in Fig. 1. As it can be observed, the GGA functional yields a nonmagnetic (due to the degeneracy between the two spin states) and metallic ground state with a finite contribution to density of states at the Fermi level. This result could be understood in a simple way by inspecting the splitting of  $d$  levels of Cu in a cubic crystal field, schematically represented in Fig. 2. On each  $\text{Cu}^{+2}$  ion, there are nine electrons placed in the  $3d$  levels. The  $d$  levels are split in the cubic crystal field into a doubly degenerate  $e_g$  (higher energy) and triply degenerate  $t_{2g}$  states (lower energy). As illustrated in Fig. 2, the metallic character and the nonmagnetic ground state is due to the degeneracy of the highest energy  $e_g$  states with either spin. On these four orbitals, Cu hosts three electrons, thus leading to partially filled bands that result in a metallic,

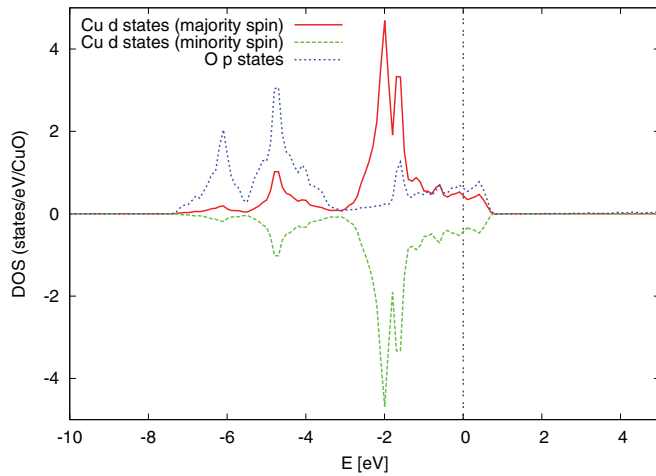


FIG. 1. (Color online) The projected density of states calculated by the GGA functional for cubic CuO.

nonmagnetic ground state. It is important to notice that O also provides a finite contribution to the density of states at the Fermi level, thus  $p$  states (nonmagnetic) are also partially filled. This scenario is similar to that of paramagnetic insulators, with the additional complication of orbital degeneracy. The orbital degeneracy contributing to the metallic character of this ground state is obviously a consequence of the cubic symmetry that makes the  $e_g$  states equivalent. This degeneracy cannot be broken by the straight use of DFT +  $U$ . The density of states of the ground state resulting from the GGA +  $U$  functional is shown in Fig. 3, where it is evident that the main effect of the Hubbard correction consists in the (probably exaggerated) stabilization of filled  $d$  states that shift to lower energies. Both  $d$  states ( $e_g$ ) and  $p$  states are left at the Fermi energy. Owing to the presence of O  $p$  states around the Fermi level, one might be tempted to extend the Hubbard correction to these states. This was indeed explored in Ref. 40. Figure 4 shows the density of states of CuO obtained with a Hubbard correction extended to O  $p$  states. The Hubbard  $U$  on O  $p$  states ( $U_p$ ) was evaluated using the same linear response method of Ref. 23 that yielded a value of  $U_p \simeq 8.47$  eV (versus 9.79 eV of Cu). As evident from the density of states, while the metallic character is preserved, a magnetic ground state now emerges from the lifting of the spin degeneracy. This unique situation is schematically illustrated in Fig. 5, where an exchange splitting between opposite spin levels has resulted in a magnetic ground state. With GGA +  $U$ , the nonmagnetic ground state results in an effective cubic symmetry, therefore the lower energy  $t_{2g}$  states are degenerate (in fact, all Cu atoms are equivalent

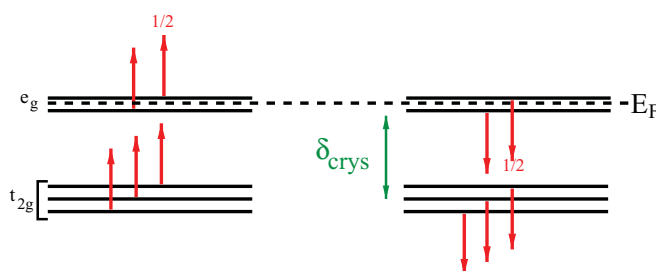


FIG. 2. (Color online) Splitting of  $d$  levels in a cubic crystal field.

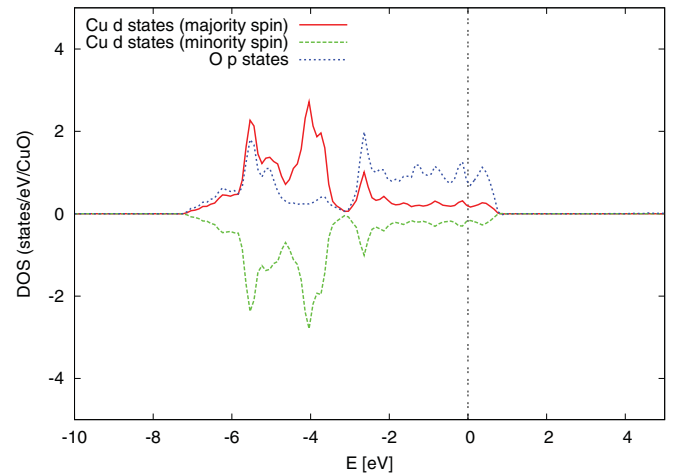


FIG. 3. (Color online) The projected density of states calculated by the GGA +  $U$  functional. The on-site Hubbard parameter is  $U = 9.79$  eV, which is calculated by the linear response approach (Ref. 23).

in spite of the rhombohedral symmetry). The rhombohedral symmetry, induced by the antiferromagnetic order, lifts this degeneracy and splits them into a nondegenerate state with  $A_{1g}$  symmetry and a doublet of  $e_g$  symmetry as illustrated in Fig. 5. However, the material is still metallic due to the degeneracy of minority-spin  $e_g$  states. It is important to notice that O  $p$  states still contribute to the metallic character (thus resulting in a partially filled  $p$  band) with equal contributions from the two spins, in spite of the polarization of the  $d$  states. The magnetic ground state in GGA +  $U + U_p$  is not directly due to  $U_p$ , but rather a consequence of the redistribution of electrons. To illustrate this point it is instructive to compare the occupations of  $d$  and  $p$  orbitals [i.e., traces of  $n_{mm}^{i\sigma}$ ,  $i$  given in Eq. (3)] between the two cases (with GGA +  $U$  and GGA +  $U + U_p$ ). For GGA +  $U$ , we obtain  $n_{Cu}^\uparrow(e_g) = n_{Cu}^\downarrow(e_g) \simeq 1.84$ , while  $n_{O_p} \simeq 4.94$ . In the case of GGA +  $U + U_p$  we obtain  $n_{Cu}^\uparrow(e_g) \simeq 1.96$ ,  $n_{Cu}^\downarrow(e_g) \simeq 1.40$ , while  $n_{O_p} \simeq 5.27$ . The main consequence of using  $U_p$  consists in the increase of  $n_{O_p}$  and the consequent

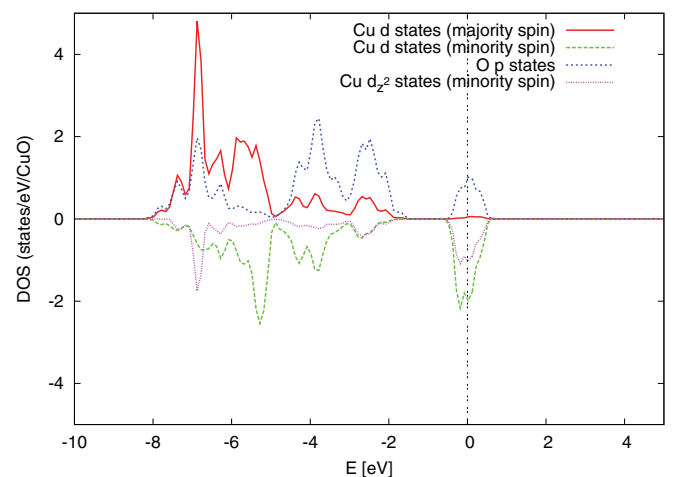


FIG. 4. (Color online) The projected density of states calculated by the GGA +  $U + U_p$  functional. The on-site Hubbard parameters are  $U = 9.79$  eV and  $U_p = 8.47$  eV, which are determined by the linear response approach (Ref. 23).

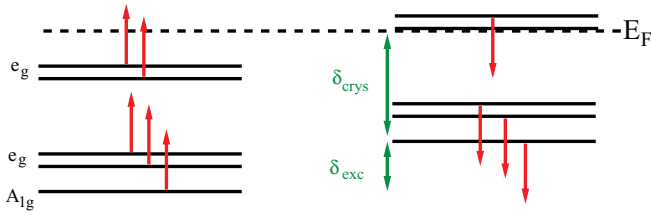


FIG. 5. (Color online) Splitting of Cu  $d$  states in a rhombohedral field with the onset of magnetic ordering.

depression of the population of the  $d$  orbitals. Thus, the magnetic ground state seems to be promoted by the partial (and numerically marginal) decrease in the population of  $d$  orbitals. This picture is corroborated by Fig. 4, which shows the explicit contribution to the density of states around the Fermi level from minority-spin  $d_{z^2}$  (one of the  $e_g$ ) states, which accounts for half of the density. It is also important to notice how the peak in the  $d_{z^2}$  density of states correlate with those of the  $p$  states, suggesting partial hybridization between Cu and O.

The emergence of the magnetic, albeit metallic, ground state is due to the rhombohedral symmetry and cannot be broken by the Hubbard corrections. Thus, the metallic character is a consequence of the crystal symmetry, similar to the case of FeO.<sup>23</sup> The effective equivalence between the  $e_g$  states dictated by the cubic or rhombohedral symmetry could be understood as effectively recovered by the superposition of two (or more) equivalent ground states (of lower symmetry) having either of the  $e_g$  orbitals occupied. To check this hypothesis and to obtain one of these states, we have set the calculation in a larger unit cell of lower symmetry. This unit cell is described by the lattice vectors given by  $\mathbf{v}_1 = (-0.5, 0.5, 0)$ ,  $\mathbf{v}_2 = (0, 1, -1)$ ,  $\mathbf{v}_3 = (0.5, 0.5, 1)$ , and contains four Cu and four O atoms. Each magnetic (111) plane contains two Cu atoms in this unit cell and they are treated as different kinds, albeit associated with the same pseudopotential. This artifact removes the effective equivalence of  $e_g$  states even for the eight-atom cell description of the cubic structure. A similar trick was also used for FeO to stabilize a broken-symmetry (orbitally ordered) phase that reproduced the structural distortions of the material under pressure.<sup>23</sup> The ground state obtained in the eight-atom cell has slightly lower energy per Cu-O pair ( $\Delta E \simeq 1.88$  eV/CuO) compared to the rhombohedral four-atom unit cell, and thus the broken-symmetry configuration is energetically favored.

It is important to remark that even in the broken-symmetry phase, an energy gap appears only if a finite Hubbard correction  $U_p$  is used on the  $O p$  states. Without a Hubbard correction on  $O p$  states, the material is predicted to be nonmagnetic and a metallic ground state still emerges from the degeneracy of the  $e_g$  orbitals with opposite spin. This correction stabilizes the  $O p$  states and increases their occupancy at the expense of lowering Cu  $d$  state occupancies. Thus, Cu  $d$  orbitals are left with nine electrons. Hund's rule magnetism favors the localization of the hole in this shell on one of the minority spin  $e_g$  states. The calculated  $d$  and  $p$  occupations reflect the localization of the hole:  $n_{\text{Cu}}^\uparrow(e_g) \simeq 2.0$ ,  $n_{\text{Cu}}^\downarrow(d_{z^2}) \simeq 0.0$ ,  $n_{\text{Cu}}^\downarrow(d_{x^2-y^2}) \simeq 1.0$ , while  $n_{O_p} = 5.51$ . These occupations also show that the Cu atoms acquire a finite magnetization which results in an AF-II ground

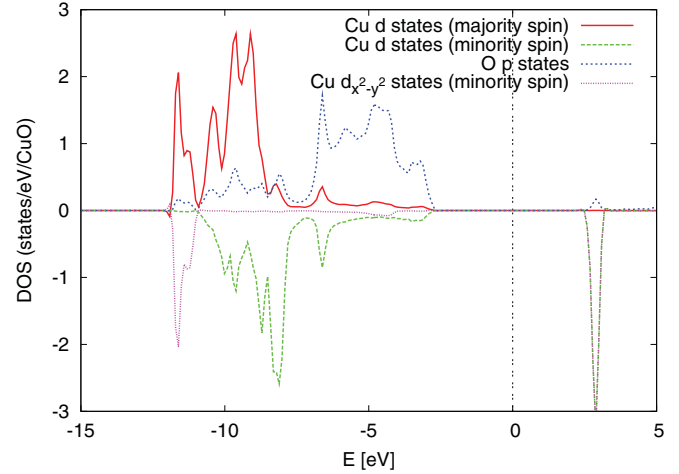


FIG. 6. (Color online) The projected density of states in the broken-symmetry phase. The on-site repulsion terms are  $U_d = 9.79$  eV and  $U_p = 8.47$  eV (calculated from the response of the GGA ground state).

state. The density of states of this ground state is shown in Fig. 6.

Although the application of a Hubbard correction  $U_p$  on noncorrelated  $O p$  states is questionable, this computational experiment is an indication of the fact that this system is characterized by a competition between two opposite tendencies: full occupation of Cu  $d$  states and the stabilization of a magnetic ground state through Hund's rule coupling. If the number of electrons on  $d$  states is lower than a certain threshold value, then the Hund's rule magnetism is dominant, otherwise a nonmagnetic ground state will appear. This competition is due to two factors: a number of  $d$  electrons between nine and ten and  $O p$  states close in energy to the  $d$  states which are able to act as a charge "reservoir" for them. It is important to remark that the conventional GGA +  $U$  functional results in a metallic and nonmagnetic ground state even in the eight-atom cell, and the system has effectively cubic symmetry. The localization of the hole in the  $d$  states of Cu, driven by  $U_p$ , breaks this effective symmetry and leads to an insulating antiferromagnetic ground state. In the next section we further test this hypothesis by an extension to the + $U$  corrective functional that explicitly includes a magnetic coupling  $J$  to encourage a magnetic ground state on each Cu atom.

#### IV. DFT + $U$ + $J$ FUNCTIONAL AND ITS APPLICATION TO THE CUBIC PHASE

The DFT +  $U$  functional introduced in Eq. (2) contains only a minimal set of on-site interaction parameters. In this section, we propose an extension of the DFT +  $U$  functional that includes magnetic (exchange) interactions (DFT +  $U$  +  $J$ ). While this is not new in literature (a review of previous approaches is given in Ref. 41), the functional we propose here deviates from previous formulations. The alternate corrective scheme can be obtained from a general second quantized

expression for electron-electron interactions [derived in Eq. (6) of Ref. 35] given by

$$\hat{V}_{\text{int}} = \frac{1}{2} \sum_{I,J,K,L} \sum_{i,j,k,l} \sum_{\sigma,\sigma'} \langle \phi_i^I \phi_j^J | V_{ee} | \phi_k^K \phi_l^L \rangle \times \hat{c}_{Ii\sigma}^\dagger \hat{c}_{Jj\sigma'}^\dagger \hat{c}_{Kk\sigma'} \hat{c}_{Ll\sigma}, \quad (4)$$

where capital letters  $\{I, \dots, K\}$  represent site indices, lowercase letters  $\{i, \dots, k\}$  represent state indices,  $\{\sigma, \sigma'\}$  are spin indices;  $V_{ee}$  denote the (screened) Coulomb interaction kernel between electrons and  $\phi_i^I$  denote the atomic wave function corresponding to state  $i$  centered on site  $I$ . The operators  $\hat{c}_{Ii\sigma}^\dagger, \hat{c}_{Ii\sigma}$  create and annihilate electrons with atomic wave function  $\phi_i^I$  and spin  $\sigma$ . Assuming that on-site interactions are dominant (especially for the localized  $d$  states of transition-metal ions) we keep only terms with  $I = J = K = L$  in the above sum. Moreover, we approximate the on-site effective interactions by the atomic averages of Coulomb and exchange terms  $U^I = \frac{1}{(2I+1)^2} \sum_{i,j} \langle \phi_i^I \phi_j^I | V_{ee} | \phi_i^I \phi_j^I \rangle$  and  $J^I = \frac{1}{(2I+1)^2} \sum_{i,j} \langle \phi_i^I \phi_j^I | V_{ee} | \phi_i^I \phi_j^I \rangle$ . As a result, we obtain

$$E_{\text{Hub}} = \sum_{I,\sigma} \frac{U^I}{2} [(n^{I\sigma})^2 + n^{I\sigma} n^{I-\sigma} - \text{Tr}[\mathbf{n}^{I\sigma} \mathbf{n}^{I\sigma}]] + \frac{J^I}{2} [\text{Tr}[\mathbf{n}^{I\sigma} \mathbf{n}^{I\sigma} + \mathbf{n}^{I\sigma} \mathbf{n}^{I-\sigma}] - (n^{I\sigma})^2], \quad (5)$$

where the occupations  $n_{ij}^{I\sigma} = \langle \hat{c}_{Ii\sigma}^\dagger \hat{c}_{Ij\sigma} \rangle$  are computed using the expression given in (3);  $n^{I\sigma} = \text{Tr}[\mathbf{n}^{I\sigma}]$  and  $n^I = \sum_{\sigma} n^{I\sigma}$ . We introduce a double-counting term to be subtracted from  $E_{\text{Hub}}$  that is evaluated as the mean-field approximation of (5) in the fully localized limit,<sup>42</sup> where each atomic orbital is either filled by a single electron or totally empty. In this approximation we have

$$\text{Tr}[\mathbf{n}^{I\sigma} \mathbf{n}^{I\sigma}] \rightarrow n^{I\sigma}, \quad \text{Tr}[\mathbf{n}^{I\sigma} \mathbf{n}^{I-\sigma}] \rightarrow n^{I\sigma_{\text{min}}},$$

where  $\sigma_{\text{min}}$  denotes the minority spin. The above expression is true for both magnetic and nonmagnetic systems (for nonmagnetic systems  $\sigma_{\text{min}} = \sigma$ , since spin-up and spin-down densities are equivalent). In the fully localized limit, the entire double-counting term thus reads

$$E_{\text{dc}} = \sum_I \frac{U^I}{2} n^I (n^I - 1) - \sum_{I,\sigma} \frac{J^I}{2} n^{I\sigma} (n^{I\sigma} - 1) + \sum_I J^I n^{I\sigma_{\text{min}}}. \quad (6)$$

The first term in the above equation is already included in the standard DFT +  $U$  functional given in Eq. (2). After some algebra, we easily obtain the expression of the corrective functional as

$$E_{\text{Hub}} - E_{\text{dc}} = \sum_{I,\sigma} \frac{U^I - J^I}{2} \text{Tr}[\mathbf{n}^{I\sigma} (\mathbf{1} - \mathbf{n}^{I\sigma})] + \sum_{I,\sigma} \frac{J^I}{2} \{\text{Tr}[\mathbf{n}^{I\sigma} \mathbf{n}^{I-\sigma}] - 2\delta^{\sigma\sigma_{\text{min}}} n^{I\sigma}\}. \quad (7)$$

Comparing (2) and (7), one can see that the on-site Coulomb repulsion parameter ( $U^I$ ) is effectively reduced by  $J^I$  for

interactions between electrons of parallel spin and a positive  $J$  term further discourages antialigned spins on the same site. As a result, the functional given in Eq. (7) encourages magnetic ordering. Within the simple Dudarev model,<sup>32</sup> the inclusion of  $J$  has only been considered as the effective renormalization of  $U$  (i.e.,  $U^I \rightarrow U^I - J^I$ ) and the terms in the second line of (7) were not included. The quadratic term in the second line of Eq. (7) can be explicated as

$$\sum_{I,\sigma} \frac{J^I}{2} n_{mm'}^{I\sigma} n_{m'm}^{I-\sigma}. \quad (8)$$

Since the occupations can be understood as the expectation value  $n_{m,m'}^{I\sigma} = \langle \hat{c}_{Im\sigma}^\dagger \hat{c}_{Im'\sigma} \rangle$ , this term describes an ‘‘orbital exchange’’ between electrons of opposite spins (e.g., up-spin electron from  $m'$  to  $m$  and down-spin electron from  $m$  to  $m'$ ). It is important to notice that this term is genuinely beyond Hartree-Fock. In fact, a single Slater determinant containing the four states  $m \uparrow, m \downarrow, m' \uparrow, m' \downarrow$  would produce no interaction term as the one above. Therefore, this contribution to the corrective functional can be understood as resulting from the interactions between configurations that differ from each other by two single-electron states. In this context, the use of occupation numbers computed as in Eq. (3) is not legitimate (these configurations do not contribute together to any single term of the electronic charge density). Thus the expression of the  $J$  term given in Eq. (7), based on a product of  $\mathbf{n}^{I\sigma}$  and  $\mathbf{n}^{I-\sigma}$ , is an approximation of a functional that would require the calculation of the two-body density matrix. Based on this reasoning, we argue that these interaction terms are not captured by approximate DFT functionals, where the total energy is a functional of the one-body electron density. Therefore, we can suppose that they are completely missing from the DFT functional and we can neglect them in the double-counting term that thus leads to

$$E_{\text{dc}} = E_{\text{dc}}^U - \sum_{I,\sigma} \frac{J^I}{2} n^{I\sigma} (n^{I\sigma} - 1), \quad (9)$$

where  $E_{\text{dc}}^U = 1/2 \sum_I U^I n^I (n^I - 1)$ . The double-counting term in Eq. (9) was previously considered in Refs. 43 and 44. It corresponds to the sum over like-spin electron pairs multiplied by the exchange parameter, and takes into account the total exchange energy in an average way. As a matter of fact, we have verified that that both dc terms (6) and (9) yield the same ground state for CuO. However, the one in Eq. (9) is numerically more stable and we have adopted it in all calculations presented here.

Although never included in corrective DFT-based functionals, terms as in Eq. (8) were introduced in numerical studies based on model Hamiltonians.<sup>45,46</sup>

In order to calculate the Hubbard exchange parameter  $J$ , we have extended the linear response approach<sup>23</sup> used in the previous section and we have computed the responses of on-site magnetizations  $m^I = n^{I\uparrow} - n^{I\downarrow}$  to a magnetic perturbation  $\beta m^I$ . Modeling the total energy of the solid with the double-counting term [either Eq. (6) or (9)], and rewriting it in terms of the on-site occupations  $n^I$  and magnetizations  $m^I$ , we can calculate the exchange parameter  $J^I$  from  $\partial^2 E / (\partial m^I)^2 = -J^I/2$ . The second derivative of the

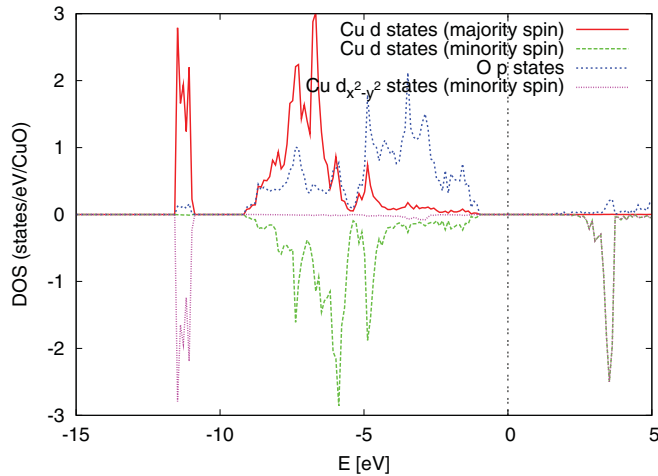


FIG. 7. (Color online) The projected density of states in the broken-symmetry phase. The Hubbard parameters for the Cu- $d$  states are  $U = 9.79$  eV and  $J = 2.50$  eV (calculated from the response of the GGA ground state).

energy with respect to on-site magnetizations are calculated using the response matrices  $\chi_{IJ} = \partial m^I / \partial \beta^J$  so that  $J^I = -2[(\chi^0)_{II}^{-1} - (\chi)_{II}^{-1}]$ . In this equation  $\chi^0$  denotes the bare response matrix which is computed from the noninteracting Kohn-Sham problem, which needs to be subtracted from the response of the interacting system to obtain the value of  $J^I$  as described in Ref. 23.

In this paper, the  $J$  parameter was computed using a 32-atom supercell and we found that  $J \simeq 2.5$  eV (the 16-atom supercell employed for the calculation of  $U$  proved to be insufficient for obtaining linearly behaving magnetic response matrices). We would like to stress that the values  $U \simeq 9.79$  eV used in the previous section and  $J \simeq 2.5$  eV are obtained by the response of the GGA ground state, and are used as “test” values in the previous and current sections. More precise values are obtained by a self-consistent procedure (i.e., by recomputing the responses using the GGA +  $U$  ground state) for the discussion of elongated structures in the next section.

In agreement with the discussion at the end of the previous section, the explicit account of magnetic interactions through the new functional results in an insulating and antiferromagnetic ground state (with a broken-symmetry phase). The resulting density of states is shown in Fig. 7. The exchange interaction parameter  $J$  enhances the splitting between opposite spin electrons and favors a magnetic (insulating) state. As can be seen in Fig. 7, the GGA +  $U$  +  $J$  functional localizes a hole in the  $d_{z^2}$  state on each Cu atom, while all other  $d$  states are filled and lie below the gap. This result suggests that the insulating ground state is stabilized by magnetic interactions. It is important to remark that this ground state is not stable in the conventional GGA +  $U$  since the on-site magnetic interactions included in the extended corrective functional of Eq. (7) play a key role in the emergence of the insulating state. Recently, the importance of the exchange coupling  $J$  in favoring metallic or insulating ground states of correlated systems has also been verified using the dynamical mean-field theory.<sup>47</sup> However, magnetic and nonmagnetic ground states are very close in energy. We hypothesize that this balance could be inverted by

doping. We have also checked that it is possible to localize the hole on the  $d_{x^2-y^2}$  orbital or a configuration with mixed occupations [i.e., one hole localized on  $d_{x^2-y^2}$  on one Cu atom and one hole localized on  $d_{z^2}$  on the other Cu atom of the same (111) plane]. These configurations have slightly higher energies than the ground state we have discussed above (the state with mixed occupations is  $\sim 0.3$  eV/cell higher in energy than the ground state, and the configuration with the  $d_{x^2-y^2}$  hole is  $\sim 0.5$  eV/cell higher in energy than the ground state). The relatively low-energy difference between them is due to symmetry that makes  $e_g$  states almost degenerate.

As pointed out in the Introduction, the broken-symmetry insulating state in the cubic phase, to the best of our knowledge, has not been found, and the degeneracy between the  $e_g$  levels was lifted through a tetragonal distortion in other works.<sup>5,8,9</sup> We have shown instead that the symmetry can be broken even for the cubic cell (with a lower-symmetry eight-atom unit cell, effectively corresponding to the cubic structure) and that an insulating state can result from magnetic interactions. In the next section, we study elongated structures and determine their ground-state properties using the eight-atom cell.

## V. TETRAGONALLY DISTORTED STRUCTURES

In this section we discuss the ground-state properties of the tetragonally distorted structures. We limit our study only to the case of AF-II ordering (unlike some previous studies,<sup>8,9</sup> which also considered other magnetic configurations) and determine the value of the tetragonal distortion  $c/a$  corresponding to lowest energy. To do so, we have calculated the Hubbard parameter  $U$  at each value of  $c/a$  between 0.9 and 1.2 using the linear response approach in a self-consistent procedure, while the  $J$  parameter was fixed to the value obtained from the cubic cell and just with the GGA response (we assumed its variation to be less important). In fact, the value of the parameter  $J$  must be calculated from the response of a nonmagnetic ground state (i.e., the GGA ground state of the cubic phase of CuO), since the linearity of the response matrices is not preserved when the ground state is magnetic (i.e., GGA +  $U$  +  $J$  ground state, or any tetragonally distorted phase). Therefore, we have limited the calculation of  $J$  to the nonmagnetic phase. The  $U$  parameters, on the other hand, are computed self-consistently until their value converges within an accuracy of  $\sim 0.2$  eV. The value of the lattice parameter  $a$  was fixed, so the volume of the cell varies between different calculations. However, we have also studied a deformation at fixed volume and obtained very similar results, which will not be discussed in this paper. In Fig. 8 we show the calculated values of Hubbard  $U$  parameter as a function of  $c/a$ . We show both the values calculated from GGA response (the green/light gray line) and the values that are calculated self-consistently (the red/gray line). The self-consistent values of the  $U$  parameters are smaller than the ones calculated from the GGA response, especially around the region close to  $c/a \sim 1$  (i.e., the cubic phase). This difference is due to the fact that the GGA ground state in the cubic structure is metallic and paramagnetic, while the GGA +  $U$  +  $J$  ground state is insulating and antiferromagnetic. This effect is also visible at large tetragonal distortions, however, it is less dramatic than for  $c/a \simeq 1$ , since GGA yields ground states that are antiferromagnetic for  $c/a \gtrsim 1.1$

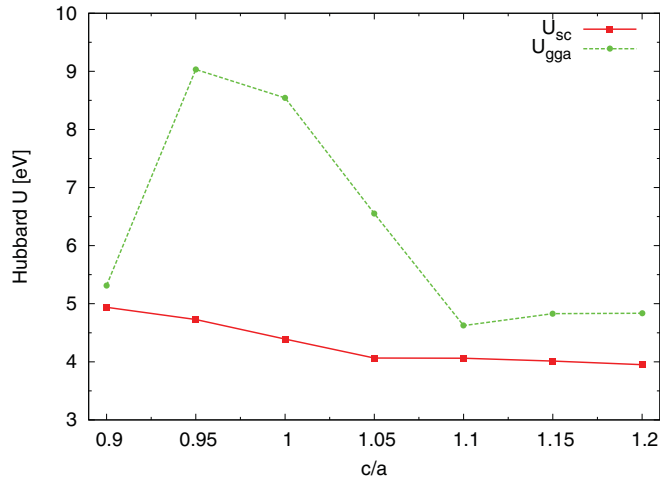


FIG. 8. (Color online) Calculated  $U_d$  for each value of  $c/a$ . The green (light gray) line shows the linear response values calculated from the GGA response and the red (gray) line shows the self-consistently calculated values.

and  $c/a \lesssim 0.9$ . From our calculations, we find that the hole in the  $d$  states of Cu atoms is localized on the  $d_{x^2-y^2}$  orbitals for  $c/a > 1$  and on the  $d_{z^2}$  orbitals for  $c/a \leq 1$ . These orbital configurations are expected, since the elongation of the  $z$  axis lowers the Coulomb repulsion energy of electrons localized on  $d_{z^2}$  orbitals. Therefore, the localization of the hole in the  $d_{x^2-y^2}$  orbitals (or, equivalently, the localization of an electron on the  $d_{z^2}$  orbitals) is energetically favorable for  $c/a > 1$  and vice versa. The minimum energy configuration was found to be at  $c/a \simeq 1.15$ , as shown in Fig. 9. The energy differences for different values of  $c/a$  are in overall agreement with the findings of previous studies.<sup>5,8</sup>

We have also calculated the energy band gaps for each structure, which lie between 1.4 eV ( $c/a = 0.9$ ) and 0.4 eV

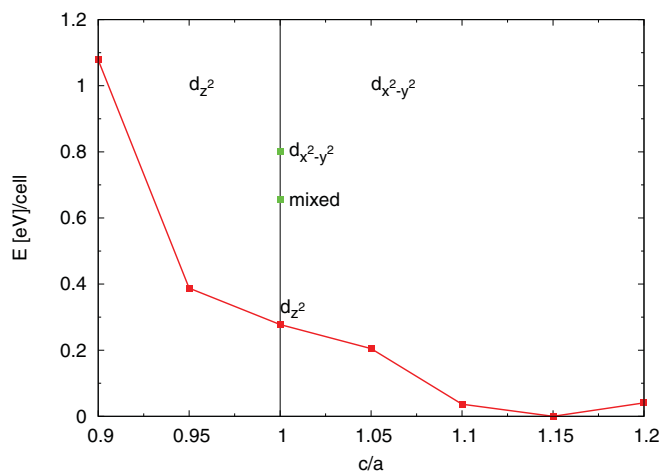


FIG. 9. (Color online) The ground-state energy profile as a function of the tetragonal distortion  $c/a$ . The orbital localizations of the holes on Cu  $d$  states for  $c/a > 1$  and for  $c/a < 1$  are labeled. The ground-state energies of different hole localizations for the cubic phase are also shown.

( $c/a = 1.2$ ) and decrease with  $c/a$ . The energy band gap for monoclinic CuO was determined to lie between 1.21 and 1.7 eV experimentally.<sup>48,49</sup> The largest value of 1.4 eV we have obtained is within the experimental range, but for larger values of  $c/a$ , the gap becomes lower than the experimental one. The difference is probably related to the fact that the structures we are considering have different symmetry than the ones studied experimentally.

The value of the tetragonal distortion we found for the most stable configuration ( $c/a \simeq 1.15$ ) is lower than the experimentally observed value of  $c/a \simeq 1.35$ . This difference could be related to the fact that our calculations do not take into account surface effects (strains) which are important for ultrathin films of tetragonal CuO grown on the SrTiO<sub>3</sub> support. Indeed, it was recently shown that when surface effects are taken into account, better agreement with experimental results is obtained.<sup>50</sup> The  $c/a$  we found is in agreement with the results of Refs. 5 and 8, however, it is lower than  $c/a \simeq 1.377$  of Ref. 9. This difference may be related to the different localization properties of the hybrid-density functionals used in Ref. 9 and DFT +  $U$ . The functional used in this paper strongly localizes the electrons on atomic sites, and is less accurate in representing hybridization effects that could be important in CuO. The disagreement could be removed with the use of the intersite interactions, which was shown to improve structural properties.<sup>35</sup> In addition, a structurally consistent calculation of the Hubbard parameters as was done in Ref. 14 is expected to result in more precise structural properties. Finally, we would like to stress that the local minimum located at  $c/a \simeq 0.95$ , which was identified in some previous works,<sup>8,9</sup> has disappeared in our calculations, as can be seen in Fig. 9. Based on our results, we think that the local minimum was the consequence of the artificially high energy of the metallic cubic phase compared to the distorted ones. We argue that the metallic state obtained with the approximate DFT functional for  $c/a = 1$  results from the degeneracy of  $e_g$  orbitals, which is the result of cubic symmetry.

## VI. SUMMARY

In this paper we have studied the electronic structure of CuO both in the cubic and tetragonal phases. We have identified the insulating state in the cubic structure, which was expected but, to the best of our knowledge, not found. The emergence of the cubic insulating state requires the breaking of symmetry in the electronic structure and leads to an orbitally ordered ground state. We have found that the insulating ground state results from a delicate balance between two tendencies: filling the  $d$  shell of Cu with (nearly) ten electrons and localizing a hole on one of the  $e_g$  states to stabilize a magnetic ground state. After stabilizing the magnetic ground states, we have identified several local energy minima in the cubic configuration (paramagnetic, with holes localized on  $d_{x^2-y^2}$  orbitals, on  $d_{z^2}$  orbitals, and with mixed types of localizations) at slightly higher energies. We have also studied tetragonal distortions in the system and found the lowest-energy configuration to be at  $c/a \simeq 1.15$ . Our findings are in reasonable agreement with experimental results, although inclusion of intersite interactions in the

functional could improve the agreement. Finally, we clarified the transition (through the cubic phase with  $c/a = 1$ ) between the two different localization regimes of Cu  $d$  electrons (on  $d_{x^2-y^2}$  orbitals for  $c/a \leq 1$  and on  $d_{z^2}$  orbitals for  $c/a > 1$ ) and suggested that the metallic state predicted by approximate DFT functionals for  $c/a = 1$  is an artifact of the degeneracy between  $e_g$  states, enforced by the symmetry of the crystal. We believe that the interplay between orbital ordering and magnetism and the interaction between the  $d$  and  $p$  electrons, highlighted in this paper, will be of interest in studying high  $T_c$  superconductors, where similar electronic dynamics and competitions between charge and

spin degrees of freedom are believed to play an important role.

#### ACKNOWLEDGMENTS

We would like to thank P. M. Grant for proposing the problem and for useful discussions. We also would like to thank Vincenzo Fiorentini for useful comments. We acknowledge support from the NSF Grant No. EAR-0810272, we thank Minnesota Supercomputing Institute for providing computational resources and technical support for this work.

- 
- <sup>1</sup>T. Kimura, Y. Sekio, H. Nakamura, T. Siegrist, and A. Ramirez, *Nat. Mater.* **7**, 291 (2008).
- <sup>2</sup>B. Yang, T. Thurston, J. Tranquada, and G. Shirane, *Phys. Rev. B* **39**, 4343 (1989).
- <sup>3</sup>S. Asbrink and L. Norrby, *Acta Crystallogr. Sect. B* **26**, 8 (1970).
- <sup>4</sup>A. Filippetti and V. Fiorentini, *Phys. Rev. Lett.* **95**, 86405 (2005).
- <sup>5</sup>P. Grant, *J. Phys.: Conf. Ser.* **129**, 012042 (2008).
- <sup>6</sup>G. Giovannetti, S. Kumar, A. Stroppa, J. van den Brink, S. Picozzi, and J. Lorenzana, *Phys. Rev. Lett.* **106**, 26401 (2011).
- <sup>7</sup>W. Siemons, G. Koster, D. Blank, R. Hammond, T. Geballe, and M. Beasley, *Phys. Rev. B* **79**, 195122 (2009).
- <sup>8</sup>G. Peralta, D. Puggioni, A. Filippetti, and V. Fiorentini, *Phys. Rev. B* **80**, 140408 (2009).
- <sup>9</sup>X. Chen, C. Fu, C. Franchini, and R. Podloucky, *Phys. Rev. B* **80**, 94527 (2009).
- <sup>10</sup>V. Anisimov, J. Zaanen, and O. Andersen, *Phys. Rev. B* **44**, 943 (1991).
- <sup>11</sup>V. Anisimov, I. Solovyev, M. Korotin, M. Czyżyk, and G. Sawatzky, *Phys. Rev. B* **48**, 16929 (1993).
- <sup>12</sup>I. Solovyev, P. Dederichs, and V. Anisimov, *Phys. Rev. B* **50**, 16861 (1994).
- <sup>13</sup>H. Hsu, P. Blaha, R. Wentzcovitch, and C. Leighton, *Phys. Rev. B* **82**, 100406 (2010).
- <sup>14</sup>H. Hsu, K. Umemoto, M. Cococcioni, and R. Wentzcovitch, *Phys. Rev. B* **79**, 125124 (2009).
- <sup>15</sup>H. Hsu, P. Blaha, M. Cococcioni, and R. Wentzcovitch, *Phys. Rev. Lett.* **106**, 118501 (2011).
- <sup>16</sup>H. Hsu, K. Umemoto, M. Cococcioni, and R. Wentzcovitch, *Phys. Earth Planet. Inter.* **185**, 13 (2010).
- <sup>17</sup>S. Stackhouse, L. Stixrude, and B. Karki, *Earth Planet. Sci. Lett.* **289**, 449 (2010).
- <sup>18</sup>S. Stackhouse, J. Brodholt, and G. Price, *Earth Planet. Sci. Lett.* **253**, 282 (2007).
- <sup>19</sup>H. Kulik, M. Cococcioni, D. Scherlis, and N. Marzari, *Phys. Rev. Lett.* **97**, 103001 (2006).
- <sup>20</sup>D. Scherlis, M. Cococcioni, P. Sit, and N. Marzari, *J. Phys. Chem. B* **111**, 7384 (2007).
- <sup>21</sup>K. Leung, I. Nielsen, N. Sai, C. Medforth, and J. Shelnut, *J. Phys. Chem. A* **114**, 10174 (2010).
- <sup>22</sup>H. Kulik and N. Marzari, *J. Chem. Phys.* **133**, 114103 (2010).
- <sup>23</sup>M. Cococcioni and S. De Gironcoli, *Phys. Rev. B* **71**, 35105 (2005).
- <sup>24</sup>I. Mazin and V. Anisimov, *Phys. Rev. B* **55**, 12822 (1997).
- <sup>25</sup>I. Solovyev, A. Liechtenstein, and K. Terakura, *J. Magn. Magn. Mater.* **185**, 118 (1998).
- <sup>26</sup>G. Mattioli, P. Alippi, F. Filippone, R. Caminiti, and A. Amore Bonapasta, *J. Phys. Chem. C* **114**, 21694 (2010).
- <sup>27</sup>A. Filippetti and N. Spaldin, *Phys. Rev. B* **67**, 125109 (2003).
- <sup>28</sup>A. Becke, *J. Chem. Phys.* **98**, 1372 (1993).
- <sup>29</sup>A. Liechtenstein and M. Katsnelson, *Phys. Rev. B* **57**, 6884 (1998).
- <sup>30</sup>S. Sharma, J. Dewhurst, N. Lathiotakis, and E. Gross, *Phys. Rev. B* **78**, 201103 (2008).
- <sup>31</sup>W. Setyawan and S. Curtarolo, *Comput. Mater. Sci.* **49**, 299 (2010).
- <sup>32</sup>S. Dudarev, G. Botton, S. Savrasov, C. Humphreys, and A. Sutton, *Phys. Rev. B* **57**, 1505 (1998).
- <sup>33</sup>D. O'Regan, N. Hine, M. Payne, and A. Mostofi, *Phys. Rev. B* **82**, 081102 (2010).
- <sup>34</sup>V. Mazurenko, S. Skornyakov, A. Kozhevnikov, F. Mila, and V. Anisimov, *Phys. Rev. B* **75**, 224408 (2007).
- <sup>35</sup>V. Campo Jr. and M. Cococcioni, *J. Phys. Condens. Matter* **22**, 055602 (2010).
- <sup>36</sup>J. Perdew, K. Burke, and M. Ernzerhof, *Phys. Rev. Lett.* **77**, 3865 (1996).
- <sup>37</sup>H. Monkhorst and J. Pack, *Phys. Rev. B* **13**, 5188 (1976).
- <sup>38</sup>M. Methfessel and A. Paxton, *Phys. Rev. B* **40**, 3616 (1989).
- <sup>39</sup>P. Giannozzi, S. Baroni, N. Bonini, M. Calandra, R. Car, C. Cavazzoni, D. Ceresoli, G. L. Chiarotti, M. Cococcioni, I. Dabo *et al.*, *J. Phys. Condens. Matter* **21**, 395502 (2009), [<http://www.quantum-espresso.org>].
- <sup>40</sup>I. A. Nekrasov, M. A. Korotin, and V. I. Anisimov, e-print [arXiv:cond-mat/0009107](http://arxiv.org/abs/cond-mat/0009107).
- <sup>41</sup>E. Ylvisaker, W. Pickett, and K. Koepernik, *Phys. Rev. B* **79**, 035103 (2009).
- <sup>42</sup>A. Petukhov, I. Mazin, L. Chioncel, and A. Liechtenstein, *Phys. Rev. B* **67**, 153106 (2003).
- <sup>43</sup>V. Anisimov, F. Aryasetiawan, and A. Liechtenstein, *J. Phys. Condens. Matter* **9**, 767 (1997).
- <sup>44</sup>M. Czyżyk and G. Sawatzky, *Phys. Rev. B* **49**, 14211 (1994).
- <sup>45</sup>J. Yoshitake and Y. Motome, e-print [arXiv:1105.5757](http://arxiv.org/abs/1105.5757).
- <sup>46</sup>D. L. H. L. Y. M. Quan and L. J. Zou, e-print [arXiv:1106.3487](http://arxiv.org/abs/1106.3487).
- <sup>47</sup>L. Medici, J. Mravlje, and A. Georges, e-print [arXiv:1106.0815](http://arxiv.org/abs/1106.0815).
- <sup>48</sup>F. Koffyberg and F. Benko, *J. Appl. Phys.* **53**, 1173 (1982).
- <sup>49</sup>F. Marabelli, G. Parravicini, and F. Salghetti-Drioli, *Phys. Rev. B* **52**, 1433 (1995).
- <sup>50</sup>C. Franchini, X. Chen, and R. Podloucky, *J. Phys. Condens. Matter* **23**, 045004 (2011).